

On the Dynamics of Piezoceramic Multilayered Bending Actuators

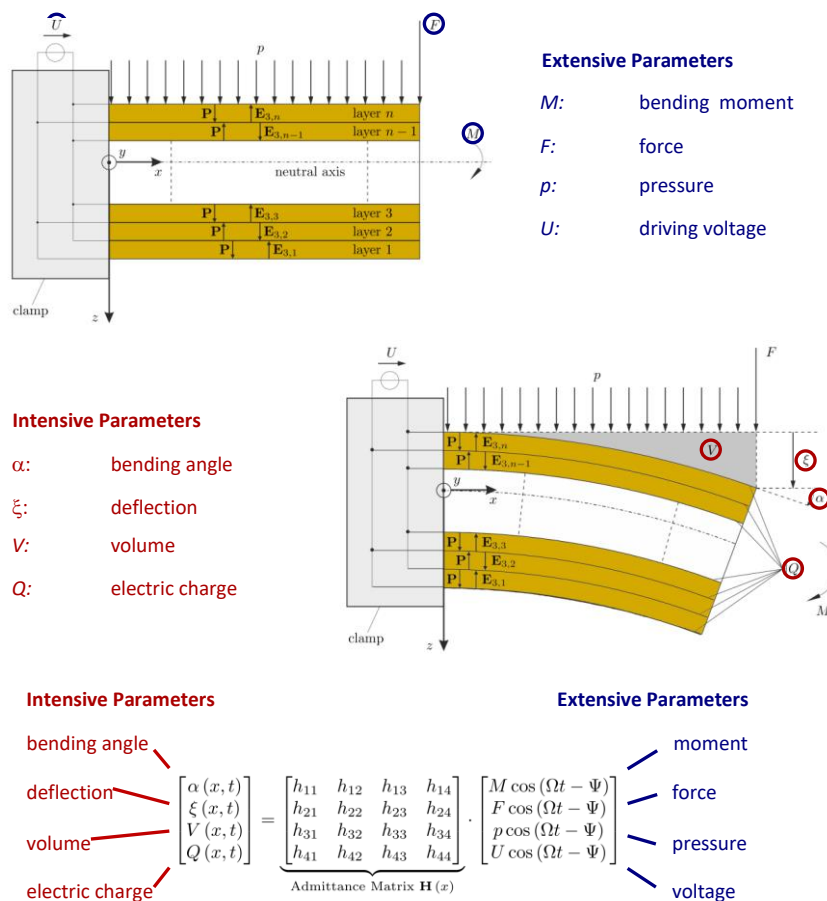
Rüdiger G. Ballas^{1*}

¹Wilhelm Büchner University of Applied Sciences, Darmstadt, D-64295, Germany

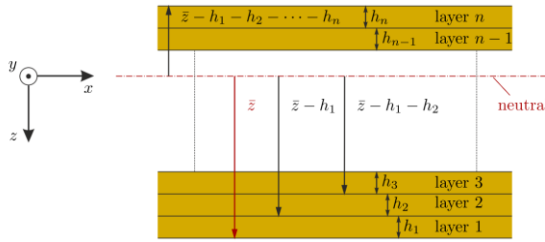
*Corresponding and Presenting Author: E-mail: ruediger.ballas@wb-fernstudium.de

DOI: 105185/vpoam-2020-0815

Graphical Abstract



Main Inertia Axis Position



$$\bar{z} = - \frac{\sum_{i=1}^n \frac{w_i}{s_{11,i}} h_i^2 - 2 \sum_{i=1}^n \frac{w_i}{s_{11,i}} h_i \sum_{j=1}^i h_j}{2 \sum_{i=1}^n \frac{w_i}{s_{11,i}} h_i}$$

- w_i : width of layer i
- h_i : height of layer i
- $s_{11,i}$: compliance of layer i
- n : number of layers

Intensive parameters with respect to a harmonic driving moment M

$$\begin{bmatrix} \alpha(x, t) \\ \xi(x, t) \\ V(x, t) \\ Q(x, t) \end{bmatrix} = \underbrace{\begin{bmatrix} h_{11} & h_{12} & h_{13} & h_{14} \\ h_{21} & h_{22} & h_{23} & h_{24} \\ h_{31} & h_{32} & h_{33} & h_{34} \\ h_{41} & h_{42} & h_{43} & h_{44} \end{bmatrix}}_{\text{Admittance Matrix } \mathbf{H}(x)} \cdot \begin{bmatrix} M \cos(\Omega t - \Psi) \\ F \cos(\Omega t - \Psi) \\ p \cos(\Omega t - \Psi) \\ U \cos(\Omega t - \Psi) \end{bmatrix}$$

$$\begin{aligned} h_{11} &= -\frac{4}{l^2 \mu} \sum_{m=1}^{\infty} X'_m(x) \frac{k_m l \alpha_M(k_m l)}{\omega_m^2 \sqrt{(1 - \eta_m^2)^2 + (2\zeta_m \eta_m)^2}} \\ h_{21} &= -\frac{4}{l^2 \mu} \sum_{m=1}^{\infty} X_m(x) \frac{k_m l \alpha_M(k_m l)}{\omega_m^2 \sqrt{(1 - \eta_m^2)^2 + (2\zeta_m \eta_m)^2}} \\ h_{31} &= -\frac{4w}{l^2 \mu} \sum_{m=1}^{\infty} \int_0^x X_m(\bar{x}) d\bar{x} \frac{k_m l \alpha_M(k_m l)}{\omega_m^2 \sqrt{(1 - \eta_m^2)^2 + (2\zeta_m \eta_m)^2}} \\ h_{41} &= -m_{\text{Piezo}} h_{11} \end{aligned}$$

$$\alpha_M(k_m l) = \frac{\sin(k_m l) \sinh(k_m l)}{\sinh(k_m l) + \sin(k_m l)}$$

Intensive parameters with respect to a harmonic driving force F

$$\begin{bmatrix} \alpha(x, t) \\ \xi(x, t) \\ V(x, t) \\ Q(x, t) \end{bmatrix} = \underbrace{\begin{bmatrix} h_{11} & h_{12} & h_{13} & h_{14} \\ h_{21} & h_{22} & h_{23} & h_{24} \\ h_{31} & h_{32} & h_{33} & h_{34} \\ h_{41} & h_{42} & h_{43} & h_{44} \end{bmatrix}}_{\text{Admittance Matrix } \mathbf{H}(x)} \cdot \begin{bmatrix} M \cos(\Omega t - \Psi) \\ F \cos(\Omega t - \Psi) \\ p \cos(\Omega t - \Psi) \\ U \cos(\Omega t - \Psi) \end{bmatrix}$$

$$\begin{aligned} h_{12} &= \frac{4}{l \mu} \sum_{m=1}^{\infty} X'_m(x) \frac{\alpha_F(k_m l)}{\omega_m^2 \sqrt{(1 - \eta_m^2)^2 + (2\zeta_m \eta_m)^2}} \\ h_{22} &= \frac{4}{l \mu} \sum_{m=1}^{\infty} X_m(x) \frac{\alpha_F(k_m l)}{\omega_m^2 \sqrt{(1 - \eta_m^2)^2 + (2\zeta_m \eta_m)^2}} \\ h_{32} &= \frac{4w}{l \mu} \sum_{m=1}^{\infty} \int_0^x X_m(\bar{x}) d\bar{x} \frac{\alpha_F(k_m l)}{\omega_m^2 \sqrt{(1 - \eta_m^2)^2 + (2\zeta_m \eta_m)^2}} \\ h_{42} &= -m_{\text{Piezo}} h_{12} \end{aligned}$$

$$\alpha_F(k_m l) = \frac{\cosh(k_m l) \sin(k_m l)}{\sin(k_m l) + \sinh(k_m l)} - \frac{\cos(k_m l) \sinh(k_m l)}{\sin(k_m l) + \sinh(k_m l)}$$

Intensive parameters with respect to a harmonic driving pressure p

$$\begin{bmatrix} \alpha(x, t) \\ \xi(x, t) \\ V(x, t) \\ Q(x, t) \end{bmatrix} = \underbrace{\begin{bmatrix} h_{11} & h_{12} & h_{13} & h_{14} \\ h_{21} & h_{22} & h_{23} & h_{24} \\ h_{31} & h_{32} & h_{33} & h_{34} \\ h_{41} & h_{42} & h_{43} & h_{44} \end{bmatrix}}_{\text{Admittance Matrix } \mathbf{H}(x)} \cdot \begin{bmatrix} M \cos(\Omega t - \Psi) \\ F \cos(\Omega t - \Psi) \\ p \cos(\Omega t - \Psi) \\ U \cos(\Omega t - \Psi) \end{bmatrix}$$

$$\begin{aligned} h_{13} &= \frac{2w}{\mu} \sum_{m=1}^{\infty} X'_m(x) \frac{\alpha_p(k_m l)}{\omega_m^2 k_m l \sqrt{(1 - \eta_m^2)^2 + (2\zeta_m \eta_m)^2}} \\ h_{23} &= \frac{2w}{\mu} \sum_{m=1}^{\infty} X_m(x) \frac{\alpha_p(k_m l)}{\omega_m^2 k_m l \sqrt{(1 - \eta_m^2)^2 + (2\zeta_m \eta_m)^2}} \\ h_{33} &= \frac{2w}{\mu} \sum_{m=1}^{\infty} \int_0^x X_m(\bar{x}) d\bar{x} \frac{\alpha_p(k_m l)}{\omega_m^2 \sqrt{(1 - \eta_m^2)^2 + (2\zeta_m \eta_m)^2}} \\ h_{43} &= -m_{\text{Piezo}} h_{13} \end{aligned}$$

$$\alpha_p(k_m l) = \frac{\cos(2k_m l)}{\sinh(k_m l) + \sin(k_m l)} - \frac{2 \cos(k_m l)}{\sinh(k_m l) + \sin(k_m l)} - \frac{2 \cosh(k_m l)}{\sinh(k_m l) + \sin(k_m l)} + \frac{2 \cos(k_m l) \cosh(k_m l)}{\sinh(k_m l) + \sin(k_m l)} + \frac{\cosh(2k_m l)}{\sinh(k_m l) + \sin(k_m l)}$$

Intensive parameters with respect to a **harmonic driving voltage U**

$$\begin{bmatrix} \alpha(x, t) \\ \xi(x, t) \\ V(x, t) \\ Q(x, t) \end{bmatrix} = \underbrace{\begin{bmatrix} h_{11} & h_{12} & h_{13} & h_{14} \\ h_{21} & h_{22} & h_{23} & h_{24} \\ h_{31} & h_{32} & h_{33} & h_{34} \\ h_{41} & h_{42} & h_{43} & h_{44} \end{bmatrix}}_{\text{Admittance Matrix } \mathbf{H}(x)} \begin{bmatrix} M \cos(\Omega t - \dots) \\ F \cos(\Omega t - \dots) \\ p \cos(\Omega t - \dots) \\ U \cos(\Omega t - \dots) \end{bmatrix}$$

$$h_{14} = m_{\text{Piezo}} h_{11}$$

$$h_{24} = m_{\text{Piezo}} h_{21}$$

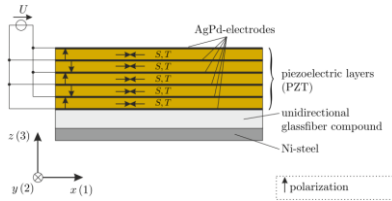
$$h_{34} = m_{\text{Piezo}} h_{31}$$

$$h_{44} = -m_{\text{Piezo}} h_{11} + \sum_{i=1}^{\infty} \frac{x w_i}{h_i} \left(\varepsilon_{33,i}^T - \frac{d_{31,i}^2}{s_{11,i}^E} \right)$$

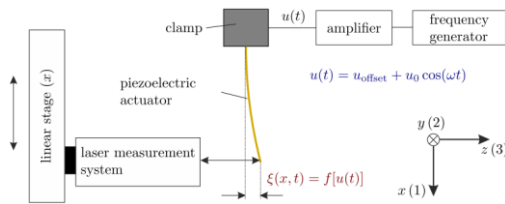
all matrix elements $h_{ij}(x)$ are determined
 experimental verification of a part of the closed form solution

deflection characteristics
 vs.
harmonic driving voltage

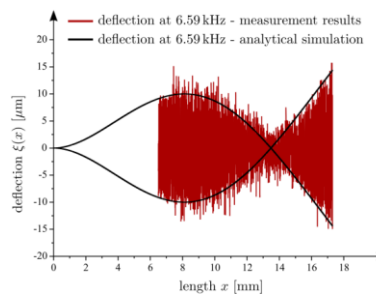
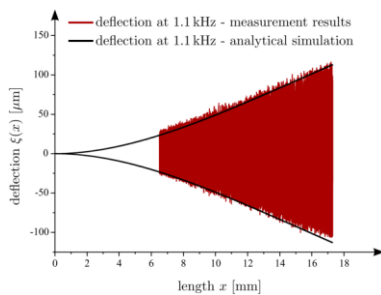
Used Multilayer Actuator and Measurement Setup



	Layer i		
	1	2	3-7
	Ni-steel	Glasfiber compound	PZT
Free length l_i (mm)	19.22	19.22	19.22
Width w_i (mm)	8.00	8.00	8.00
Thickness h_i (μm)	100	200	5 x 48
Compliance $s_{11,i}^E$ ($10^{-12} \text{ m}^2/\text{N}$)	6.369	11.364	14.144
Piezoelectric Coefficient $d_{31,i}$ (10^{-12} m/V)	-	-	-350



Measured and Calculated Deflection Characteristics (1st and 2nd Vibration Mode)



Abstract

In this lecture the derivation of the dynamic constituent equations for any kind of clamped-free piezoelectric multilayer bending actuators under different excitation conditions formulated generally for any point over the entire length l of the actuator is demonstrated. The constituent equations are presented by a 4x4 dynamic admittance matrix $\mathbf{H}(x)$ which combines the dynamic extensive parameters mechanical moment M at the free end of the bending actuator, force F applied perpendicularly to the tip of the bending actuator, uniform pressure load p applied over the entire length of the bending actuator and applied electric voltage U with the dynamic intensive parameters angular deflection α , deflection ξ , volume displacement V , and electric charge Q . All calculations are based on the neutral axis position \bar{z} of a multilayered cantilever. In recent publications the dynamic characteristics of piezoelectric laminate cantilever structures only have been described for bimorphs and triple layer piezoelectric benders without taking the aspects of the equivalent viscous damping and the different vibration modes into account. Both aspects are indispensable for the physical description of the resonance behaviour of piezoelectric cantilevers. For experimental investigations a specially developed piezoelectric multilayer bending actuator consisting of high-effective piezoceramics (layer thickness $\sim 48 \mu\text{m}$) is used. In order to verify a part of the closed form solution of the dynamic admittance matrix of piezoelectric multilayer bending actuators the emphasis is laid on the experimental determination of the dynamic deflection characteristics for the first two vibration modes over nearly the entire length of the actuator as a function of the dynamic driving voltage U . The experimental results are compared to the analytical calculations based on the 4x4 matrix $\mathbf{H}(x)$.

Keywords: piezoelectric bending actuator; multilayer; dynamic admittance matrix; constituent equations; closed form solution.

References

1. J. G. Smits, *Journal of Microelectromechanical Systems*, **1994**, 3, 105-112.
2. A. Ballato, *IEEE Transactions on Ultrasonics, Ferroelectrics and Frequency Control*, **1991**, 38, 595-602.
3. N. Rogacheva, C. C. Chou, S. H. Chang, *IEEE Transactions on Ultrasonics, Ferroelectrics and Frequency Control*, **1998**, 45, 285-294.
4. Q. Wang, S. T. Quek, *Smart Materials and Structures*, **2000**, 9, 10-109.
5. R. G. Ballas, H. F. Schlaak, A. J. Schmid, *Sensors and Actuators A: Physical*, **2006**, 130-131, 91-98.

Biography of Presenting Author



Rüdiger G. Ballas holds the professorship for electrical engineering at Wilhelm Büchner University of Applied Sciences Darmstadt, Germany. In addition to his activity as vice dean of the department of engineering sciences at Wilhelm Büchner University, his research activities focus in particular on piezoelectric materials, sensors and actuators as well as on piezoelectric energy harvesting and (micro-) electromechanical systems (MEMS). Before his university career he held leading positions in research and development at different companies concerned with piezoelectric sensors and actuators. He earned his doctorate degree at Technical University Darmstadt, Germany for his research work in the field of piezoelectric multilayered bending actuators.

During his pre-doctoral studies he already received several awards for outstanding work in the field of microstructuring of quartz crystals for high-frequency applications in modern telecommunications technologies. Furthermore, in 2017 he received the IAAM Medal due to notable and outstanding contribution in the field of “New Age Technology & Innovations”, Stockholm, Sweden. He is author of various publications and author/co-author of several textbooks published by the renowned publisher Springer Nature. Besides amateur astronomy, his passionate hobbies include playing acoustic fingerpicking/fingerstyle guitar and singing.

Citation of Video Article

Vid. Proc. Adv. Mater., Volume 1, Article ID 200815 (2020)

Full Video Article <https://www.proceedings.iaamonline.org/article/vpoam-2020-0815>